Developmental and Comparative Immunology 52 (2015) 58–68

Contents lists available at ScienceDirect

Developmental and Comparative Immunology

journal homepage: www.elsevier.com/locate/dci

Characterization of a *MAVS* ortholog from the Chinese tree shrew (*Tupaia belangeri chinensis*)

Ling Xu [a], Dandan Yu [a], Li Peng [a,b], Yu Fan [a,b], Jiaqi Chen [c], Yong-Tang Zheng [a,c], Chen Wang [d], Yong-Gang Yao [a,b,c,*]

[a] *Key Laboratory of Animal Models and Human Disease Mechanisms of the Chinese Academy of Sciences & Yunnan Province, Kunming Institute of Zoology, Kunming, Yunnan 650223, China*
[b] *Kunming College of Life Science, University of Chinese Academy of Sciences, Kunming, Yunnan 650204, China*
[c] *Kunming Primate Research Center of the Chinese Academy of Sciences, Kunming Institute of Zoology, Chinese Academy of Sciences, Kunming 650223, China*
[d] *State Key Laboratory of Cell Biology, Institute of Biochemistry and Cell Biology, Shanghai Institutes for Biological Sciences, Chinese Academy of Sciences, Shanghai, China*

ARTICLE INFO

Article history:
Received 21 March 2015
Revised 20 April 2015
Accepted 22 April 2015
Available online 27 April 2015

Key words:
MAVS
Tree shrew
Antiviral innate immunity
Evolutionary conservation

ABSTRACT

Human mitochondrial antiviral signaling protein (hMAVS, also known as IPS-1, VISA, or Cardif) is essential for antiviral innate immunity. The Chinese tree shrew (*Tupaia belangeri chinenses*), a close relative of primates, is emerging as a potential animal model for investigating viral infection. However, there is a lack of biological knowledge about the antiviral innate immunity of the tree shrew. In this study, we identified and characterized the function of the Chinese tree shrew *MAVS* gene (*tMAVS*). The cDNA of *tMAVS* was 2771 bp in length and encoded a polypeptide of 501 amino acids. Phylogenetic analyses based on the amino acid sequences revealed a closer affinity of tMAVS with those of primates. Quantitative real-time PCR analysis indicated that *tMAVS* mRNA was constitutively expressed in all seven tissues analyzed in this study. The *tMAVS* mRNA expression was rapidly and significantly increased after RNA virus infections. Ectopic-expression of tMAVS significantly potentiated the virus-triggered activation of IRF3, NF-κB and interferon-β (IFN-β), whereas knockdown of tMAVS displayed the opposite effect. Furthermore, tMAVS mutants lacking the caspase activation and recruitment (CARD) domains or the transmembrane (TM) domain were unable to induce IFN-β. Similar with hMAVS, mitochondrial localization of tMAVS was dependent on its domain. Collectively, this study revealed evolutionary conservation of the MAVS antiviral signaling pathway in the Chinese tree shrew.

© 2015 Elsevier Ltd. All rights reserved.

1. Introduction

The tree shrew (*Tupaia belangeri*), a squirrel-like small mammal, has a wide distribution in Southeast Asia and Southwest China (Peng et al., 1991). Because of its unique characteristics, such as small body size, high brain-to-body mass ratio, short reproductive cycle and life span, low-cost of maintenance, and a close relationship to primates (Fan et al., 2013; Xu et al., 2013a), the tree shrew has been proposed as a viable experimental animal for making human disease models, especially for infectious diseases (Xu et al., 2013b). Previous studies have found that tree shrew is susceptible to infection with different human viruses, including hepatitis C virus (Amako et al., 2010; Xu et al., 2007), hepatitis B virus (Kock et al., 2001; Yan et al., 1984, 1996), influenza virus (Yang et al., 2013), herpes simplex virus (Rosen et al., 1985), Coxsackie virus A16 (Li et al., 2014) and EV71 (Wang et al., 2012). However, there are many lacunae, including low efficiency of infection and unknown mechanism of virus infection in this species, need to be further explored.

The innate immune system is the first line of defense against virus infection and of key importance early in viral infections. The cytoplasmic sensor of viral RNA is mainly mediated by the members of retinoic acid-inducible gene I (RIG-I) like receptor family (RLRs). The RLR family contains three members: RIG-I (retinoic acid-inducible gene I), MDA5 (melanoma differentiation-associated gene 5) and LGP2 (laboratory of genetics and physiology 2) (Kato et al., 2006). Activation of RIG-I and MDA5 by viruses is coupled to mitochondrial antiviral signaling gene (MAVS, also known as IPS-1, Cardif or VISA) (Kawai et al., 2005; Meylan et al., 2005; Seth et al., 2005; Xu et al., 2005) through CARD:CARD domain interactions (Potter et al., 2008), which finally causes the induction of antiviral and inflammatory response mediated by IFN-β and NF-κB signaling (Belgnaoui et al., 2011). MAVS contains an N-terminal CARD domain, a

* Corresponding author. Kunming Primate Research Center of the Chinese Academy of Sciences, Kunming Institute of Zoology, Chinese Academy of Sciences, Kunming 650223, China. Tel.: +86 871 65180085; fax: +86 871 65180085.
E-mail address: yaoyg@mail.kiz.ac.cn (Y.-G. Yao).

http://dx.doi.org/10.1016/j.dci.2015.04.014
0145-305X/© 2015 Elsevier Ltd. All rights reserved.

proline-rich region (PRR) in the middle, and a C-terminal transmembrane domain (TM). This protein was initially reported to localize to mitochondria to exert its function (Seth et al., 2005), and also localized to peroxisomes and mitochondrial-associated endoplasmic reticulum membrane (MAM) (Dixit et al., 2010; Horner et al., 2011). Peroxisomal MAVS has been shown to be involved in the early antiviral response, whereas mitochondrial MAVS was implicated at a later point to promote type I interferon (IFN) and interferon-stimulated gene (ISG) expression (Dixit et al., 2010). MAM-localized MAVS directs innate immunity against HCV (Horner et al., 2011). The functional differences among mitochondria-, peroxisome-, and MAM-localized MAVS suggest that this protein recruits distinct downstream components and set up a very powerful network in innate immune response. Knowledge of the innate immune recognition of viral infection in tree shrew may finally help the development of animal models for human diseases.

In this study, we identified and characterized a MAVS ortholog from the Chinese tree shrew. We demonstrated that tMAVS has an ability to suppress various viral replications through activation of the IRF3/7 and NF-κB-dependent IFN responses.

2. Materials and methods

2.1. Experimental animals

The Chinese tree shrews were purchased from the experimental animal core facility of the Kunming Institute of Zoology (KIZ), Chinese Academy of Sciences (CAS). After lethally anesthetized by diethyl ether, we collected seven different tissues (heart, liver, spleen, lung, kidney, intestine and brain) from 10 animals. Tissue samples were quickly dissected and directly frozen in liquid nitrogen. All experimental procedures were performed according to the guidelines approved by the Ethics Committee of KIZ (Approval No: SYDW20110315001).

2.2. Total RNA extraction and reverse-transcription (RT)

Total RNA was extracted from different tissues and primary renal cells of the tree shrew using RNAsimple Total RNA Kit (TIANGEN) according to the manufacturer's instructions. The A260/A280 ratio of total RNA was measured on a biophotometer (Eppendorf) and only these samples with a value of 1.8–2.0 were used for subsequent reverse-transcription. We also evaluated the quality and integrity of RNA samples based on the 28S and 18S rRNA bands on a 1% agarose gel. One microgram total RNA was used to synthesize cDNA by using oligo-dT_{18} primer and M-MLV reverse transcriptase (Promega).

2.3. Reverse transcription quantitative real-time PCR (RT-qPCR)

RT-qPCR was performed using the SYBR green Premix Ex Taq II (TaKaRa, Dalian) supplemented with gene specific primers on a MyIQ2 Two-Color Real-Time PCR Detection system (Bio-Rad, USA). The thermal cycling protocol was 1 cycle at 95 °C for 1 min, followed by 40 cycles of 95 °C for 15 s and 55 °C for 15 s. The resultant PCR products were analyzed by the Bio-Rad software (Bio-Rad, USA). In brief, a volume of 20 μL containing 0.4 μM of each upstream and downstream primer (Table 1), 1 μL of cDNA prepared from different tissues, and 10 μL of 2 × SYBR green Premix Ex Taq II was used for the RT-qPCR reaction. The gene expression levels were analyzed using the relative standard curve method. All quantifications were normalized to the tree shrew *β-actin* and were analyzed using the GraphPad software (GraphPad Software, La Jolla, CA, USA).

2.4. Identification and cloning of tree shrew MAVS

PCR primers for amplification of *tMAVS* were designed (Table 1) based on the predicted *MAVS* sequences of the tree shrew retrieved from the Ensembl (http://www.ensembl.org/index.html) and the genome information of the Chinese tree shrew that was described in our recent study (Fan et al., 2013) and the newly established tree shrew database (http://www.treeshrewdb.org) (Fan et al., 2014). PCR amplification was performed in a volume of 20 μL reaction mixture containing 1 μL cDNA containing 0.4 μM of each primer, 4 mmol/L Tris–HCl (pH 8.3), 1 mmol/L $MgCl_2$, 20 mmol/L KCl, 80 μM of each dNTP, and one unit of LA Taq polymerase (TaKaRa). Amplification started with a denaturation cycle at 95 °C for 1 min, followed by 35 cycles of 30 s at 94 °C, 30 s at 55 °C, and ended with a final extension cycle for 2 min at 72 °C. PCR products were purified on spin columns and directly sequenced using Big Dye Terminator v3.1 Cycle Sequencing Kit (Applied Biosystems) on an automated sequencer (ABI PRISM 3730XL, Applied Biosystems) at the Kunming Biodiversity Large-Apparatus Regional Center, KIZ.

Table 1
Primers and vectors used in this study.

Primer	Sequence (5′–3′)	Restriction endonuclease	Application and vector
tMAVS-qF	AGCATGGTGCCCCCCAAGGT	–	Analytical RT-qPCR
tMAVS-qR	AGGTAAGCCCTGGCTGCCTC	–	
tIFN-β-qF	ACCACTTGGAAACCATGC	–	Analytical RT-qPCR
tIFN-β-qR	TTTCCACTCGGACTATCG	–	
tMAVS-F	ATGTCATTTGCCGAGAAC	–	Fragment amplification
tMAVS-R	CTGGAGTGGGCGCCGCCG	–	
tMAVS-5′RACE	CTGCTGTGTGGGGACTGTCT	–	5′ RACE
tMAVS-3′RACE-1	CCCATCAACTCTGCACGTG	–	3′ RACE
tMAVS-3′RACE-2	AGCCTGGGCTTGTATCCCACTCCAC	–	3′ RACE nested
tMAVS-Bgl-F	GA***AGATCT***ATGTCATTTGCCGAGAAC	*Bgl* II	PCR for constructing tMAVS-EGFP using pEGFP-N2 vector
tMAVS-Kpn-R	GG***GGTACC***CTGGAGTGGGCGCCGCCG	*Kpn* I	
tMAVS-ΔCARD-F	AAGACCTATAAGTCCTGCGAACTGTC	–	PCR for constructing mutant tMAVS without the CARD domain using tMAVS-EGFP vector
tMAVS-ΔCARD-R	GACAGTTCGCAGGACTTATAGGTCTT	–	
tMAVS-ΔTM-F	GTGTGTCAGGGTTCGGCGGCGCCCAC	–	PCR for constructing mutant tMAVS without the TM domain using tMAVS-EGFP vector
tMAVS-ΔTM-R	GTGGGCGCCGCCGAACCCTGACACAC	–	
tIFN-β-pro.-Kpn-F1	GG***GGTACC***TTTGCTTTCCTTTGCTTTG	*Kpn* I	PCR for constructing IFN-β-Luc using pGL3-Basic vector
tIFN-β-pro.-Nhe-R	GGAATTC***GCTAGC***CCTTCCTCCATGGGCATGG	*Nhe* I	
tMAVS-BamH-F	CGC***GGATCC***ATGTCATTTGCCGAGAAC	*BamH* I	PCR for constructing tMAVS-3Tag-6 using pCMV-3Tag-6 vector
tMAVS-Hind-R	CCC***AAGCTT***CTGGAGTGGGCGCCGCCG	*Hind* III	

Restriction endonuclease sites introduced by PCR are underlined.
RT-qPCR, quantitative real-time PCR.

The complete cDNA sequence was obtained via 5′ and 3′ RACE using the SMARTer™ RACE cDNA Amplification Kit (Clontech) and 3′ Full RACE Core Set Ver.2.0 (TaKaRa), respectively. All primers were listed in Table 1. Purified PCR products were cloned into the PMD 19-T simple vector (TaKaRa). Five positive clones of each insert were sequenced.

2.5. Evolutionary analyses

To infer the phylogenetic position of the Chinese tree shrew based on the *MAVS* sequences, we retrieved the *MAVS* mRNA sequences of 11 species from GenBank: *Macaca mulatta* (Rhesus monkey), NM_001042666.1; *Gorilla gorilla* (Western gorilla), XM_004061754.1; *Callithrix jacchus* (white-tufted-ear marmoset), XM_002747412.2; *Homo sapiens* (human), NM_020746.4; *Canis familiaris* (dog), NM_001122609.1; *Bos taurus* (cow), NM_001046620; *Mus musculus* (house mouse), NM_001206385.11; *Rattus norvegicus* (Norway rat), NM_001005556.1; *Sus scrofa* (pig), NM_001097429.1; *Oryctolagus cuniculus* (Rabbit), XM_002710888.1; *Pan troglodytes* (chimpanzee), XM_525410.2. Both the coding DNA sequences (CDS) and amino acid sequences were used for the phylogenetic analyses. Amino acid sequence alignment was performed using Muscle 3.7 (Edgar, 2004) with the guidance of aligned protein sequences. The dog (*Canis familiaris*) was used as the outgroup to root the phylogenetic tree. Trees were reconstructed according to the neighbor-joining (NJ) method and the maximum likelihood (ML) by MEGA5.0 (Tamura et al., 2011).

2.6. Plasmid construction

For epitope-tagged tMAVS constructs, PCR fragment was cloned into pEGFP-N2 with *Bgl* II and *Kpn* I and into FLAG-tagged pCMV-3Tag-6 with *BamH* I and *Hind* III. Truncated tMAVS proteins lacking the putative N-terminal CARD domain (residues 11–77) and the transmembrane (TM) domain (residues 475–497) were generated by multi-sites directed mutagenesis (Stratagene). The tree shrew *IFNB1* promoter luciferase reporter (IFN-β-Luc) was constructed by using primers (Table 1) with the *Kpn* I and *Nhe* I sites that amplified region –259 to +26 of the promoter and the pGL3-basic luciferase reporter vector (Promega). All constructs were verified by sequencing.

2.7. Cell culture

HEK293 and Vero cells were grown in DMEM supplemented with 10% FBS and 1 × penicillin/streptomycin (Invitrogen, USA) at 37 °C in 5% CO2. Primary renal cells were prepared and cultured as described in our recent study (Yu et al., 2014).

2.8. Virus infection

Sendai virus (SeV) and vesicular stomatitis virus (VSV) were kind gifts from Dr. Xinwen Chen of Wuhan Institute of Virology, CAS. Herpes simplex virus-1 (HSV-1) was introduced from Dr. Jumin Zhou's lab at KIZ. Avian influenza virus (AIV) and Newcastle disease virus (NDV) were obtained from China Institute of Veterinary Drug Control. SeV, AIV and NDV were propagated by injecting 10-day-old specific-pathogen-free embryonated chicken egg with stocks of virus that were diluted in phosphate-buffered saline (PBS). The 50% tissue culture infective dose ($TCID_{50}$) of VSV was determined by green fluorescence, and the titers of HSV-1, AIV and NDV were determined by cytopathic effect. The titers were calculated by the Reed–Muench method. The titer of SeV was determined by hemagglutination test on chicken erythrocytes.

Primary tree shrew renal cells were incubated with NDV (MOI = 10), AIV (MOI = 10), VSV (MOI = 0.01), SeV (20 HAU/mL) or HSV-1 (MOI = 10) for 1 h in DMEM without FBS, respectively, then cells were rinsed and cultured in fresh medium containing 1% FBS for the indicated times before the harvest.

2.9. Luciferase reporter assay

HEK293 cells or tree shrew renal cells were plated in 48-well plates at a density of 1×10^4 cells and cultured overnight. Cells were transfected with 0.1 μg of a Luciferase reporter vector (pGL3-tIFN-β, pNFκB-TA-Luc (Clontech), or ISRE cis-reporter (Stratagene)), together with 0.01 μg pRL-SV40-*Renilla* (Promega; as an internal control), the indicated amounts of an empty vector (Mock) or expression constructs using Lipofectamine™ 2000. The transfected cells were left untreated or infected with SeV (20 HAU/mL) or NDV (MOI = 10) for 12 h. Cells were lysed and detected for luciferase activity by using the Dual-Luciferase Reporter Assay System (Promega) on an infinite M1000 Pro multimode microplate reader (Tecan).

2.10. Immunofluorescence analysis

The tree shrew primary renal cells were seeded on glass coverslips and grown overnight to 40% confluence in DMEM medium supplemented with 10% FBS (Invitrogen, USA) at 37 °C in 5% CO2. Thirty-six hours after transfection with indicated vectors, cells were left untreated or infected with SeV (20 HAU/mL) for 12 h. For immunofluorescence analysis, cells were fixed with 4% paraformaldehyde for 10 min and were incubated with the rabbit anti-VISA (1:500, Sigma-Aldrich) to detect endogenous tMAVS. Mouse anti-Flag (1:1000, Abmart) was used to detect the Flag-tagged indicated proteins overnight at 4 °C. After three washes with PBS, cells were incubated with the secondary antibody (1:500, Life Technologies) for 1 h. Nuclei was stained with DAPI (Roche). Intact cells were imaged by using an Olympus FluoView™ 1000 confocal microscope (Olympus).

2.11. Western blotting and native PAGE

HEK293 cells and primary renal cells were seeded in 6-well plates at 70% confluence and were transfected with plasmids using X-tremeGENE HP DNA Transfection Reagent (Roche). Cells were lysed on ice in RIPA lysis buffer (Beyotime). Cell lysates were centrifuged at 12,000 *g* at 4 °C for 5 min, then were subjected to 12% SDS–PAGE and transferred onto polyvinylidene fluoride (PVDF) membranes (Roche) using standard procedures. The membranes were blocked with 5% nonfat dry milk in Tris buffered saline (TBS) containing 0.1% Tween 20 (TBST) at room temperature for 2 h. Then the membranes were incubated with particular primary antibody overnight at 4 °C (anti-EGFP (1:2000, Enogene) to detect tMAVS-EGFP and its mutants; rabbit anti-VISA (1:1000, Sigma-Aldrich) to detect endogenous tMAVS; mouse anti-Flag (1:5000, Abcam) to detect Flag-tagged indicated proteins; mouse anti β-actin (1:10,000, Enogene) to detect the tree shrew and human β-actin). Membranes were washed three times with TBST for 5 min each and were incubated with anti-mouse or anti-rabbit secondary antibody (1:10,000, KPL, USA) for 1 h at room temperature. The proteins were detected using enhanced chemiluminescence (ECL) reagents (Millipore). Native PAGE was performed as previously described (Iwamura et al., 2001).

2.12. Statistical test

Comparisons between different groups were conducted by using Student's *t* test (PRISM software, GraphPad Software, Inc., CA, USA). Data are presented as mean ± SEM. A P value <0.05 was considered to be significantly different.

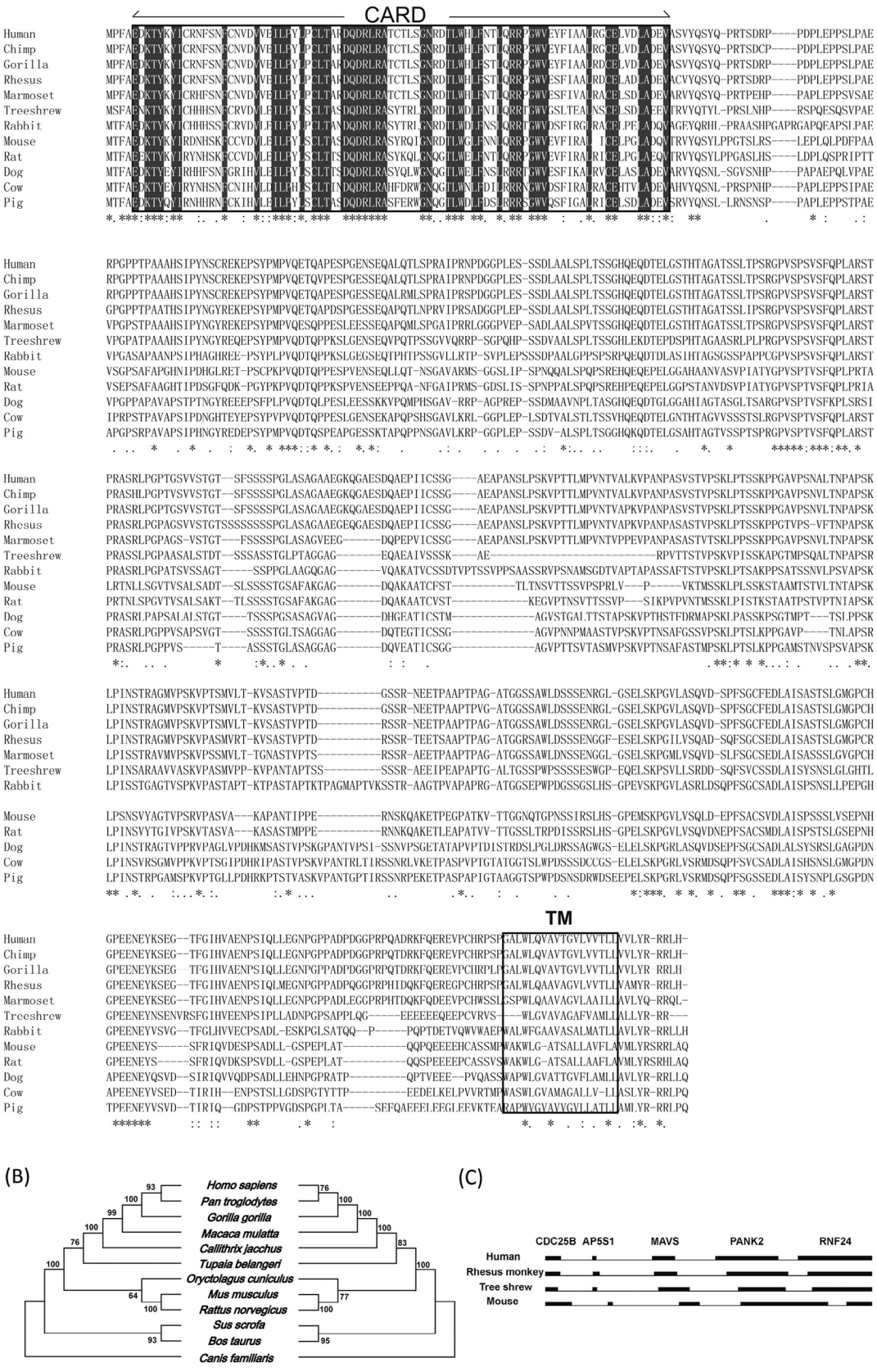

Fig. 1. Sequence comparison and evolutionary analysis of the *MAVS* gene. (A) Alignment of the MAVS protein sequences of the Chinese tree shrew and other vertebrates. The CARD and the transmembrane (TM) domains were marked in the alignment. The conserved CARD region was marked in black, and the residues of the TM region as predicted by the TMpred server (http://www.ch.embnet.org/software/TMPRED_form.html) were boxed. (B) Neighbor-joining (left) and maximum likelihood (right) trees of the MAVS protein sequences of 11 vertebrate species (GenBank accession numbers are listed in Section 2). (C) Conserved synteny around the *MAVS* gene in the genomic sequences of the Chinese tree shrew, mouse, monkey and human (data are retrieved from the assemblies at the Ensembl website [http://www.ensembl.org/] and the tree shrew genome generated in our previous study [http://www.treeshrewdb.org]).

3. Results

3.1. cDNA cloning and sequence analysis of tMAVS

According to the predicted *MAVS* gene sequence of the tree shrew in Ensembl and the tree shrew genome sequence generated by our own (Fan et al., 2013, 2014), we inferred that the *tMAVS* gene was composed of 6 exons. The full-length of *tMAVS* transcript had a length of 2771 bp (GenBank accession number KM005100), with a 151 bp 5′-UTR and a 1114 bp 3′-UTR (without a poly(A) tail). The open reading frame (ORF) consisted of 1506 bp and encodes 501 amino acids. Similar to human ortholog of MAVS, tMAVS contained 3 canonical functional domains: an N-terminal CARD domain, a proline rich (PRR) domain and a C-terminal TM domain. Multiple sequence alignment showed that the CARD domain of the tree shrew had the highest protein sequence identity (72%) to that of human. The TM domain was less conserved than the CARD domain and shared 60% amino acid sequence identity with human ortholog (Fig. 1A).

To gain an insight into MAVS evolution, an NJ tree was constructed using the MAVS amino acid sequences of 11 representative mammalian species. We observed a clustering pattern consistent with the recognized species tree, as reported in our previous study (Fan et al., 2013). In particular, the tree shrew showed a close relationship to the primates in the NJ tree (Fig. 1B, left). We observed a similar clustering pattern when the ML approach was used (Fig. 1B, right). We further searched the conserved synteny of MAVS and other markers in the genomic region. We identified 3 markers in region where the *tMAVS* gene was located, and these syntenies were conserved in a variety of mammals (Fig. 1C), reinforcing the notion that *tMAVS* is a true ortholog.

3.2. Expression analysis of tMAVS

Constitutive mRNA expression of *tMAVS* was observed in the heart, liver, spleen, lung, kidney, small intestine and brain. Heart and kidney had a relatively high mRNA expression, whereas small intestine had the lowest mRNA expression (Fig. 2A). In the tree shrew primary renal cells, *tMAVS* expression increased upon infection of RNA virus or DNA virus. Infection with AIV, VSV, SeV, NDV or HSV-1 led to the highest level of *tMAVS* mRNA expression at 3 h or 6 h post-infection, followed by a decline of *tMAVS* mRNA level (Fig. 2B). tMAVS protein level was increased at 9 h after the infection of these viruses (Fig. 2C). There was a decrease of tMAVS upon viral infection at 3 h after the infection, although the mRNA was significantly increased at this time point. Overall, *tMAVS* exhibited similar expression properties to that of mammalian orthologs upon viral infections and was constitutively expressed in tree shrew primary renal cells.

3.3. tMAVS activated ISRE, NF-κB and IFN-β luciferase reporters

To determine the role of tMAVS in innate immunity, we constructed tMAVS expression vectors and explored its function in activating the ISRE, NF-κB and IFN-β luciferase reporters. As expected, ectopic-expression of tMAVS activated IFN-β-Luc reporter and potentiated the SeV-induced activation of the IFN-β-Luc in a dose-dependent manner in the tree shrew primary renal cells (Fig. 3A), which required coordinative and cooperative function of IRF3 and NF-κB (Tamura et al., 2008). Consistently, tMAVS could activate both the ISRE-Luc and NF-κB-Luc. It also potentiated the SeV-induced activation of the ISRE-Luc and NF-κB-Luc in a dose-dependent manner (Fig. 3A). Furthermore, over-expression of tMAVS in HEK293 cells markedly potentiated the SeV-induced IRF3 dimerization (Fig. 3B), which was a hallmark of IRF3 activation (Zhong et al., 2008). Since hMAVS over-expression was sufficient to delay the replication of VSV (Seth et al., 2005), we next determined

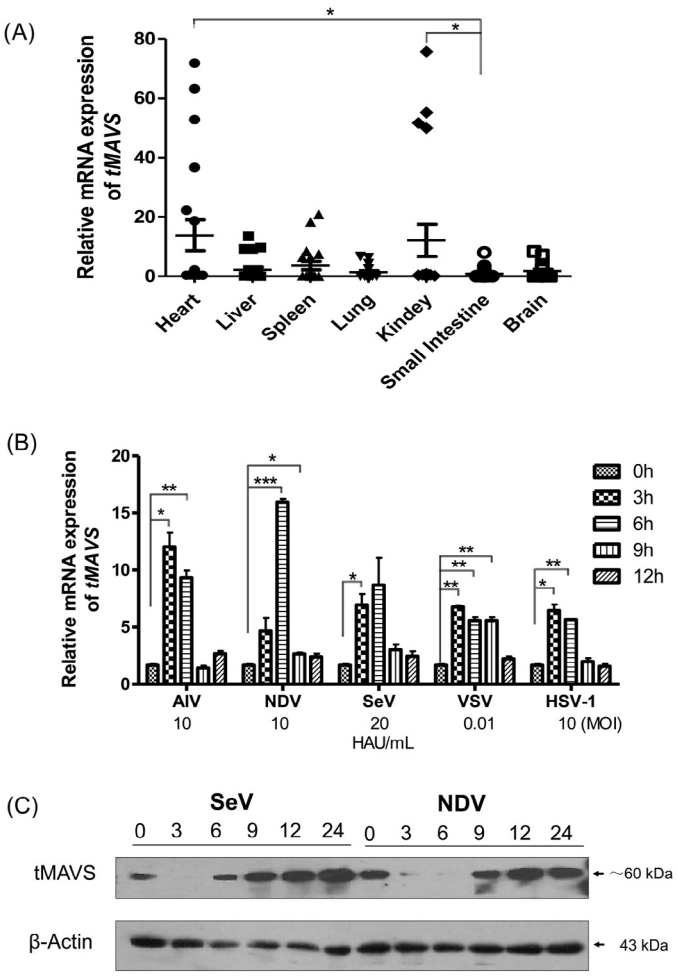

Fig. 2. Expression of tMAVS in tree shrew tissues and renal cells upon virus infections. (A) *tMAVS* mRNA expression levels in seven tissues from the Chinese tree shrew (N = 10). The *β-actin* was used for quantification of *tMAVS* mRNA expression level. (B) Up-regulation of the *tMAVS* mRNA expression after challenging with different viruses in the tree shrew primary renal cells. Cells were harvested at the indicated times after infection with different viruses [AIV – avian influenza virus (MOI = 10), VSV – vesicular stomatitis virus (MOI = 0.01), SeV – Sendai virus (20 HAU/mL), NDV – Newcastle disease virus (MOI = 10), HSV-1 – Herpes simplex virus-1 (MOI = 10)] and were analyzed for *tMAVS* mRNA expression relative to *β-actin*. (C) Immunoblot of endogenous tMAVS and β-actin in the tree shrew primary renal cells that were infected with SeV (20 HAU/mL) and NDV (MOI = 10) for the indicated times. Endogenous tMAVS was detected using an anti-VISA antibody. Data are representative of three independent experiments. $^{*}P < 0.05$, $^{**}P < 0.01$, $^{***}P < 0.001$, Student's *t* test. Bars represent mean ± SEM.

whether tMAVS could mediate a similar effect in the tree shrew cells. As indicated by the diminished GFP expression, ectopic-expression of tMAVS inhibited GFP-tagged VSV replication (Fig. 3C). These results suggested that tMAVS played a critical antiviral role in the tree shrew.

3.4. tMAVS was required for virus-triggered IFN-β promoter activation

We further investigated the knockdown effect of endogenous tMAVS in virus-triggered IFN signaling. We used siRNA for tMAVS (tMAVS-siRNA) that could substantially inhibit endogenous tMAVS expression at the mRNA and protein levels (Fig. 4A). As shown in Fig. 4B, sitMAVS substantially inhibited the IFN-β promoter activity and potentiated SeV-induced activation of the IFN-β-Luc. Furthermore, knockdown of tMAVS inhibited NDV- and

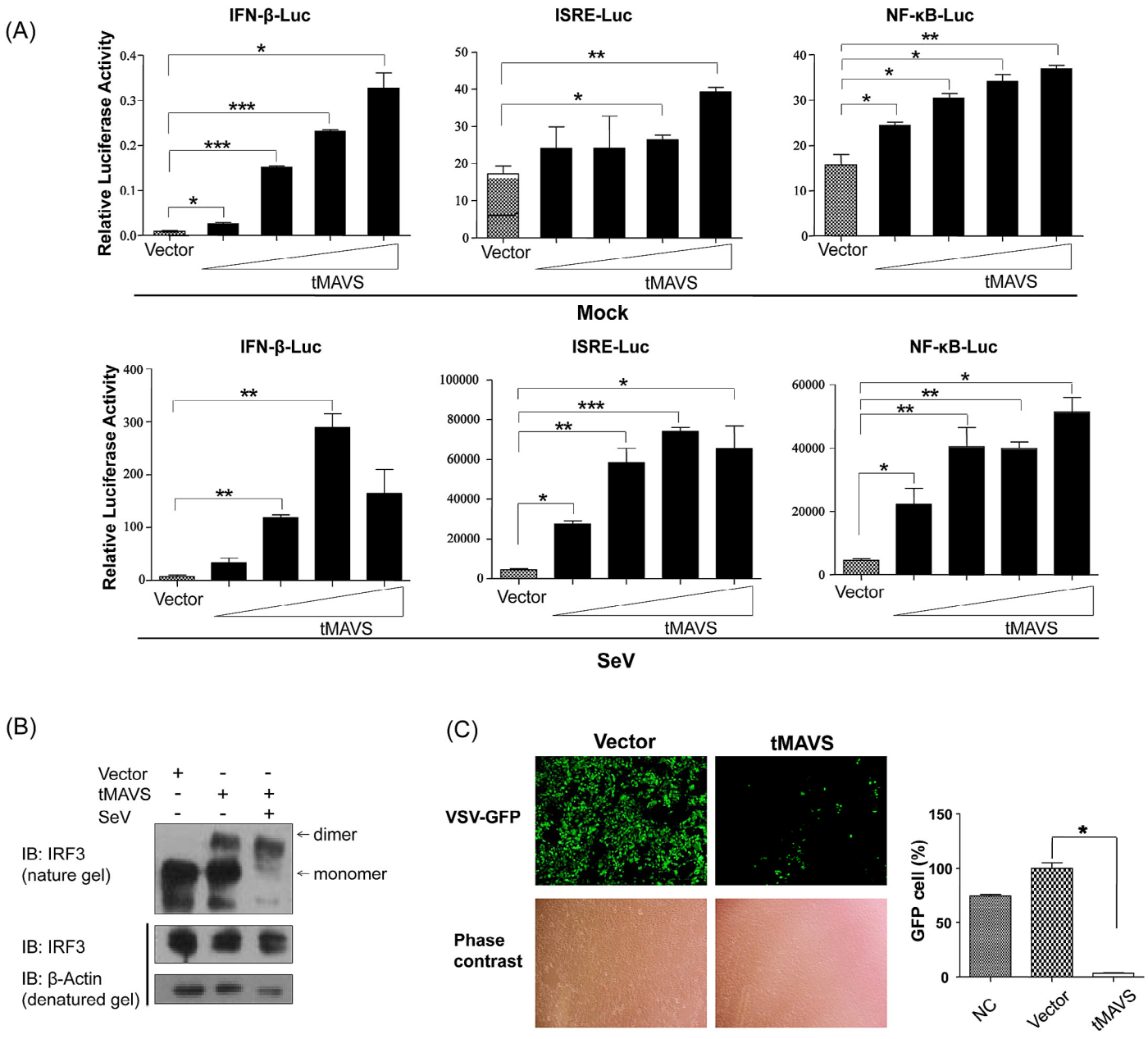

Fig. 3. Effect of over-expression of tMAVS in cells with and without virus infections. (A) tMAVS activated the IFN-β, ISRE and NF-κB luciferase reporters in a dose-dependent manner. The tree shrew primary renal cells (1×10^5) were transfected with the respective reporter vector and increased amount of tMAVS expression vector (tMAVS-3Tag-6 vector) for 36 h, then were left uninfected or infected with SeV (20 HAU/mL) for 12 h before the harvest for luciferase assay. (B) Over-expression of tMAVS activated SeV-induced IRF3 activation. HEK293 cells (2×10^5) were transfected with an empty vector or tMAVS expression vector for 24 h, then were infected with or without SeV for 12 h. Cell lysates were separated by native (upper panel) or 12% SDS–PAGE (bottom panel) and were analyzed with the indicated antibodies. (C) Over-expression of tMAVS inhibited vesicular stomatitis virus (VSV) replication. The tree shrew primary renal cells were transfected with the empty vector (pCMV-3Tag-6 vector), tMAVS expression vector for 12 h, followed by infection with VSV-GFP for 12 h. Cells were photographed under an Olympus microscopy (original magnification ×10). Percentage of VSV-GFP positive cells was quantified by flow cytometry. The GFP percentage of tMAVS expression vector was normalized to controls (empty vector). $^{*}P < 0.05$, $^{**}P < 0.01$, $^{***}P < 0.001$, Student's t test. Bars represent mean ± SEM. All experiments were repeated for three times with similar results.

SeV-induced transcription of endogenous *tIFNB1* gene (Fig. 4C), and significantly enhanced VSV replication (Fig. 4D). These results suggested that tMAVS was required for efficient cellular antiviral responses.

3.5. *The CARD-like domain and TM domain were essential for tMAVS signaling*

The N-terminal CARD-like and TM domains of MAVS were evolutionarily conserved (Fig. 1A). To determine the functions of these domains, we created expression constructs encoding MAVS mutant proteins lacking either the CARD-like domain (ΔCARD) or the TM domain (ΔTM) (Fig. 5A). As shown in Fig. 5, deletion of the CARD-like domain or the TM domain decreased the ability of MAVS to activate the ISRE, NF-κB and IFN-β promoters. Moreover, these mutants inhibited the activation of ISRE, NF-κB and IFN-β promoters by NDV. Especially, MAVS-ΔCARD completely lost its ability to activate NF-κB in response to NDV (Fig. 5C, right). Thus, the CARD-like domain and TM domain of tMAVS were essential for downstream tMAVS signaling.

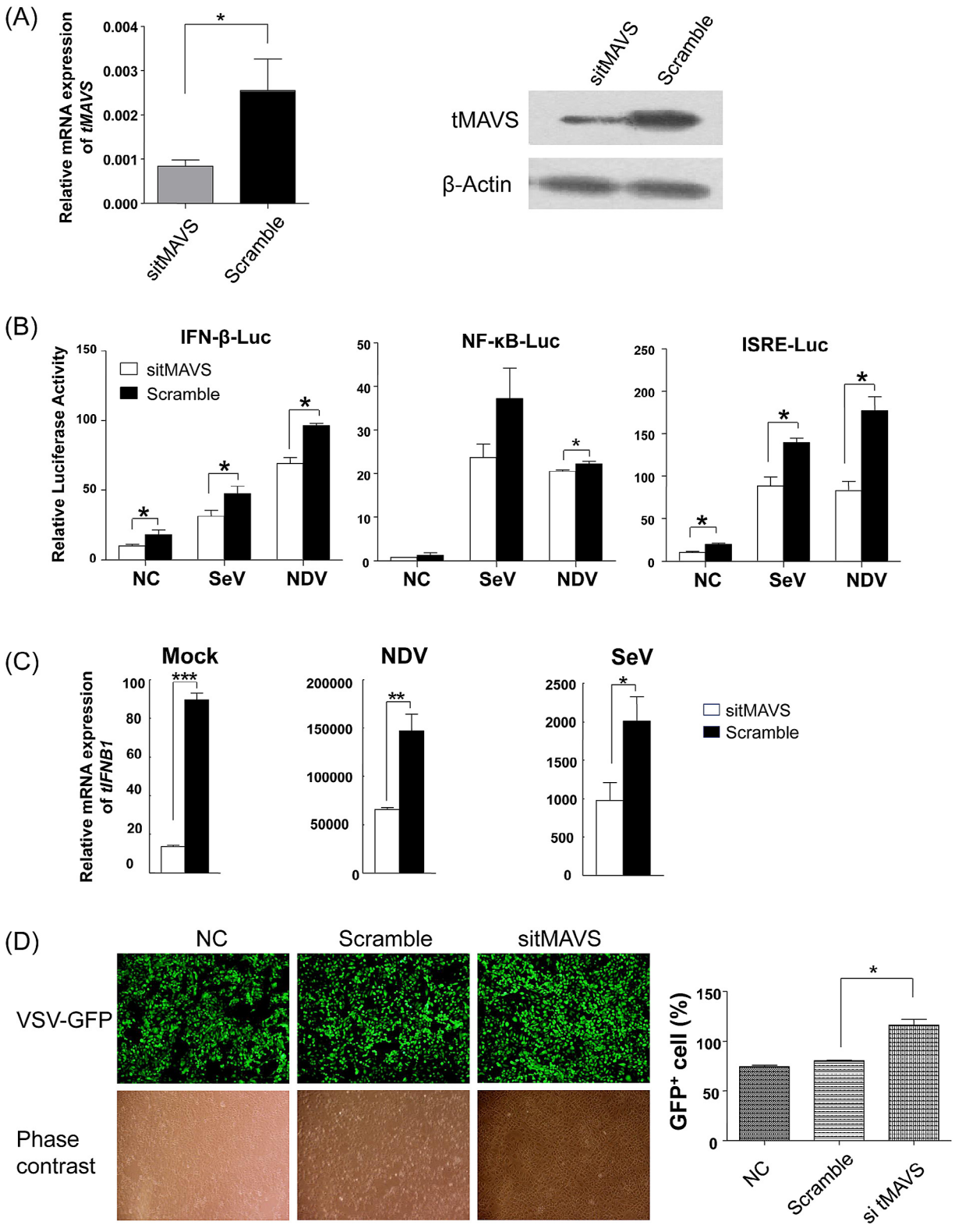

Fig. 4. tMAVS was required for virus triggered IFN-β promoter activation. (A) Effects of tMAVS-siRNA (sitMAVS) on endogenous expression of *tMAVS* mRNA (left) and protein (right). The tree shrew primary renal cells (1×10^5) were transfected with siRNA negative control (Scramble, 50 nM) or the sitMAVS (50 nM). Cells were harvested at 24 h after transfection and cell lysates were analyzed for tMAVS protein and mRNA expression. Knockdown of tMAVS caused an inhibition of virus-induced IFN-β-Luc, ISRE-Luc and NF-κB-Luc activation (B) and significant decrease of tree shrew *tIFNB1* mRNA expression (C). The tree shrew primary renal cells (1×10^5) were transfected with the siRNA negative control (Scramble, 50 nM) or sitMAVS (50 nM) for 24 h, followed by infection with or without the indicated viruses for 12 h before the harvest. (D) Knockdown of tMAVS increased VSV replication. The tree shrew primary renal cells (1×10^5) were transfected with the siRNA negative control (Scramble, 50 nM) or sitMAVS (50 nM) for 12 h, followed by infected with VSV-GFP (MOI = 0.01) for 12 h. A panel of cells without any treatment was used as the control. Cells were quantified for VSV-GFP production by flow cytometry. $^*P < 0.05$, $^{**}P < 0.01$, $^{***}P < 0.001$, Student's *t* test. Bars represent mean ± SEM. All experiments were repeated three times with similar results.

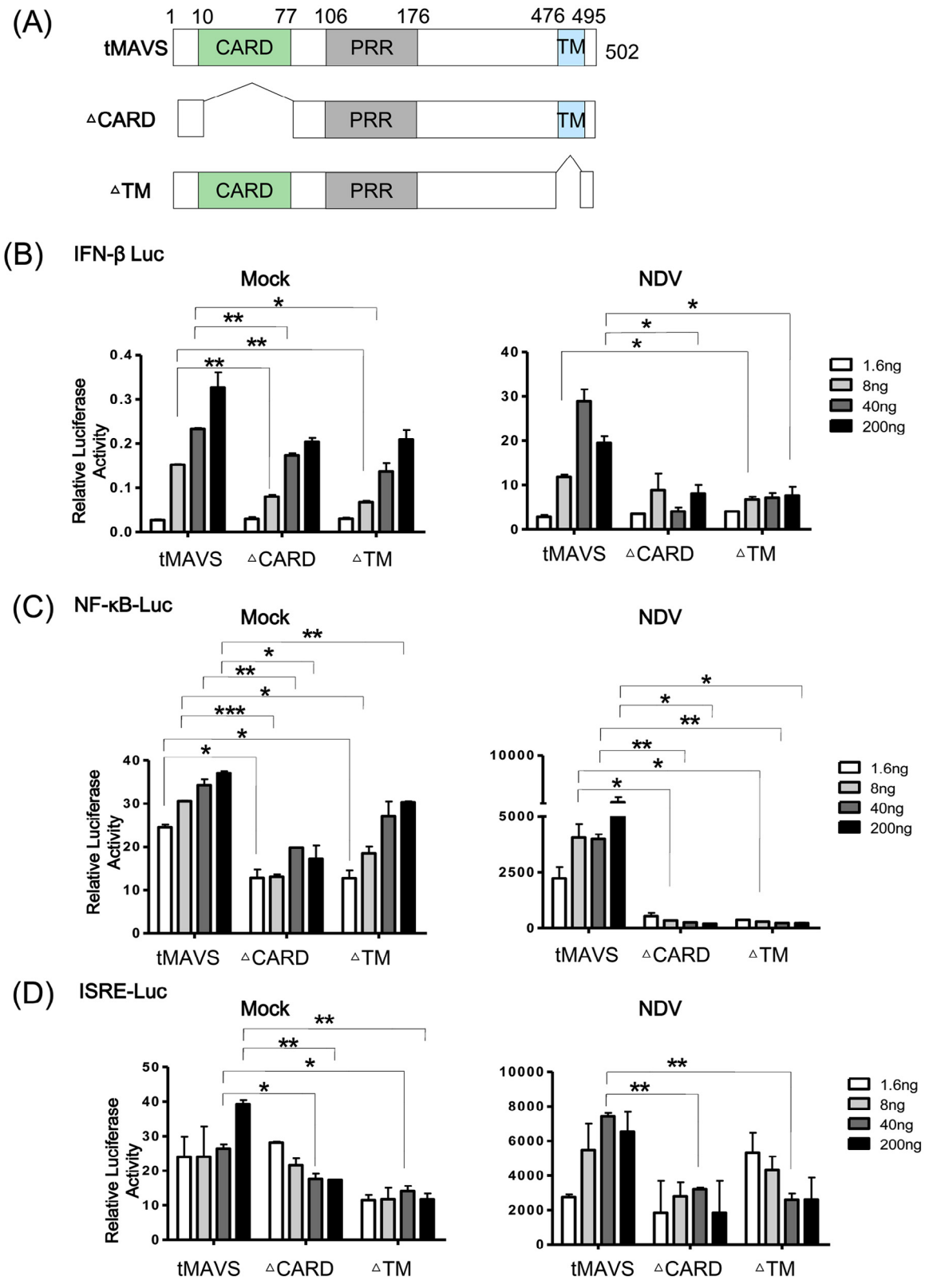

Fig. 5. The CARD-like domain was essential for tMAVS signaling. (A) A diagram illustrating the MAVS mutants. ΔCARD: lacking residues 11–77; ΔTM: lacking residues 475–497. Activation effect of tMAVS on the IFN-β-Luc (B), NF-κB-Luc (C) and ISRE-Luc (D) in HEK293 cells was dependent on the CARD and TM domains. Cells were co-transfected with the respective luciferase vector and the expression vector for tMAVS or its mutants for 24 h, then were left uninfected (mocked) or infected with NDV for 9 h before the harvest for luciferase assays. $^{*}P < 0.05$, $^{**}P < 0.01$, $^{***}P < 0.001$, Student's t test. Bars represent mean ± SEM. All luciferase assays were performed three times with similar results.

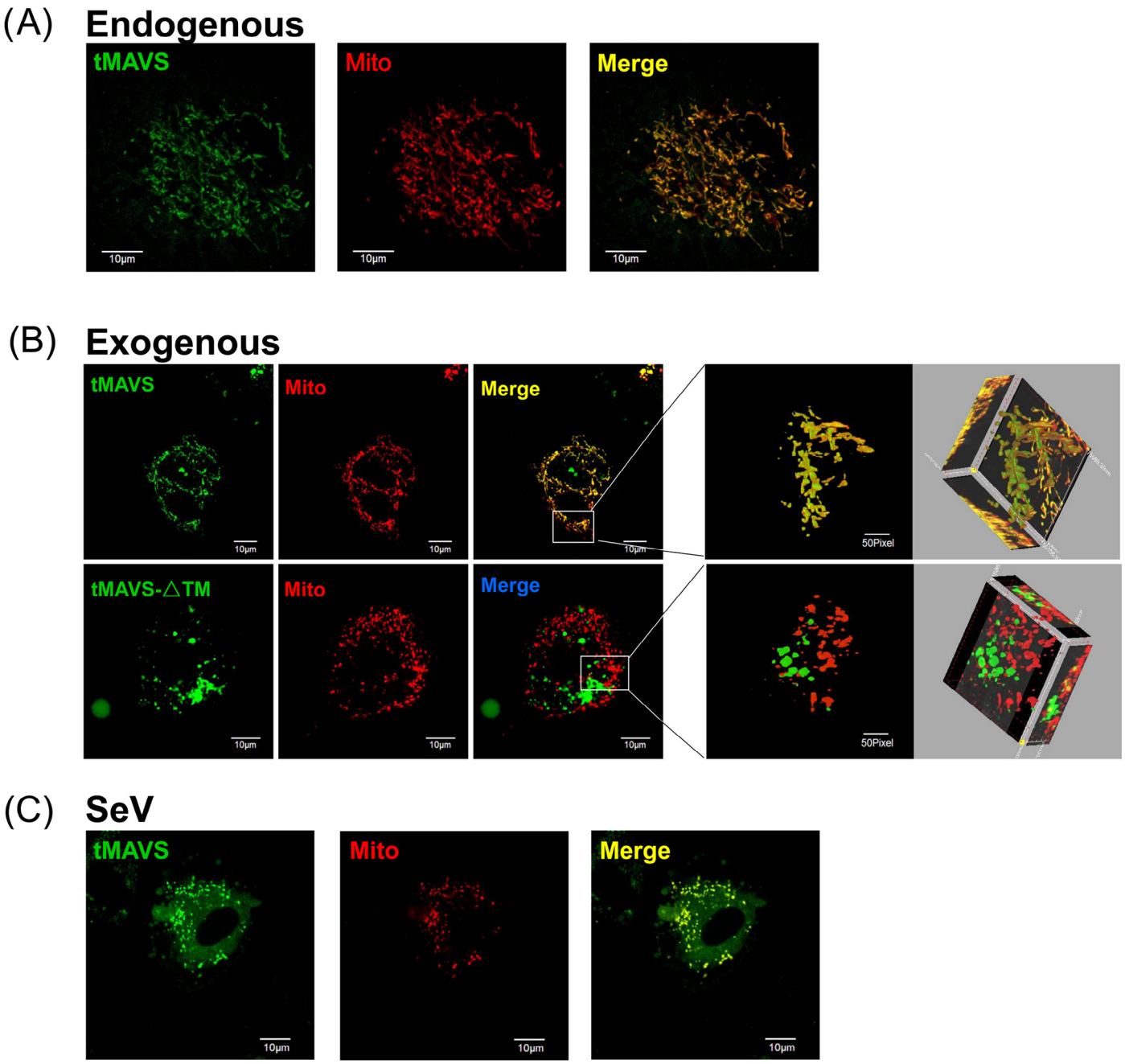

Fig. 6. Subcellular localization of endogenous and exogenous tMAVS. (A) tMAVS was a mitochondrial protein. Endogenous tMAVS was immune-stained to show the co-localization of tMAVS with mitochondria in the tree shrew primary renal cells. (B) Localization of ectopic-expressed tMAVS to mitochondria was dependent on its TM domain. Deletion of the TM domain (ΔTM) blocks the translocation of tMAVS into mitochondria. The 3D pictures were constructed by using an Olympus FluoView™ 1000 confocal microscope (Olympus). (C) Formation of puncta-like tMAVS particles in the tree shrew primary renal cells infected with SeV for 12 h. For both (B) and (C), tMAVS-EGFP (the wild-type or the ΔTM mutant) and pDsRed-Mito were co-transfected (concentration ratio 10:1) into primary renal cells for 48 h, which were then imaged by confocal microscopy. The yellow staining in the overlay image indicates a co-localization of tMAVS and pDsRed-Mito. (For interpretation of the references to color in this figure legend, the reader is referred to the web version of this article.)

3.6. Cellular localization of tMAVS

The distribution of MAVS in the mitochondria is vital for its role in signaling (Kawai et al., 2005; Meylan et al., 2005; Seth et al., 2005; Xu et al., 2005). Confocal microscopy was used to analyze the subcellular localization of the tMAVS. We found that the green fluorescent tMAVS (endogenous) was clearly merged with the red fluorescent mitochondria in primary renal cells (Fig. 6A). Exogenous tMAVS proteins were exclusively co-localized with mitochondria in the three-dimensional images (Fig. 6B, upper). However, deletion of the TM domain in tMAVS disrupted the mitochondrial localization, suggesting that mitochondrial localization was dependent on its TM domain (Fig. 6B, lower). After SeV infection, tMAVS appeared to form a dot distribution in the mitochondria (Fig. 6C), which was consistent with a previous report for a redistribution of hMAVS and the formation of densely packed, speckled MAVS puncta in virus-infected mouse embryonic fibroblasts (Xu et al., 2014).

4. Discussion

MAVS acts as an adaptor molecule that bridges the interactions between RIG-I/MDA5 sensing of different classes of viruses and downstream signaling (Takeuchi and Akira, 2010). The *MAVS* gene has been characterized in several species, including pig (Wang et al., 2008), fish (Biacchesi et al., 2009; Simora et al., 2010; Su et al., 2011), chicken (Liniger et al., 2012); all these studies showed a conservation of MAVS. In our recent study of the genome of the Chinese tree shrew, a rising biomedical research model animal, we found that tree shrews lost RIG-I (DDX58) (Fan et al., 2013), which functions to recognize various RNA virus and trigger the transduction cascade involving MAVS in the signaling pathway. Under such a condition, whether the function of MAVS still conserves in the tree shrew is an open question. In this study, we aimed to characterize the MAVS homolog in tree shrew. We cloned the full-length cDNA sequence of *tMAVS* and performed sequence comparison analysis. Our results showed that tMAVS shared many canonical structure hallmarks with human and other mammalian MAVS proteins. tMAVS had a close affinity with that of primates (Fig. 1B), which was consistent with the recognized species tree based on whole genome information (Fan et al., 2013). Over-expression of tMAVS led to activation of the ISRE, NF-κB and IFN-β luciferase reporters, and concomitantly induced a strong antiviral ability against VSV in primary renal cells (Fig. 2). Knockdown of endogenous tMAVS showed opposite effects (Fig. 3). These observations proved that the function of tMAVS was homologous to that of other mammalians.

The function of tMAVS was dependent on its TM and CARD domains, although the TM region of tMAVS exhibited relatively low protein sequence similarity (60%) compared with hMAVS (Fig. 1A). The tMAVS mutant lacking TM domain impaired its ability to activate the ISRE, NF-κB and IFN-β (Fig. 5) and mitochondrial localization (Fig. 6B). These results were consistent with the observation that the TM domain was essential for both IFN induction and MAVS localization to mitochondrial outer membrane in mammalian (Seth et al., 2005). Similarly, over-expression of the tMAVS mutant lacking the CARD domain abated its ability to activate the ISRE, NF-κB and IFN-β promoter reporters (Fig. 5), which provided direct evidence for an essential role of this domain for the tMAVS function. Taken together, our results indicated the CARD and TM domains were essential for tMAVS-mediated signaling and tMAVS was evolutionarily and functionally conserved in the Chinese tree shrew.

It is suggested that tMAVS played a role in the early stage of innate antiviral immune response (Kawai et al., 2005; Meylan et al., 2005; Seth et al., 2005; Xu et al., 2005). Upon RNA or DNA virus infection, *tMAVS* mRNA expression in the tree shrew primary renal cells was significantly up-regulated at 3 h after the infection and returned back to basal level at 12 h post-infection (Fig. 2B). Unexpectedly, stimulation with SeV and NDV caused a trough of the tMAVS protein expression level in early period of infection (Fig. 2). Similar tendency was also observed in previous reports (Seth et al., 2005; Xu et al., 2005). The exact cause of this pattern and its biological implications remained unknown. This pattern might reflect posttranscriptional and posttranslational regulation of RLR signaling pathway to inhibit excessive immunological and inflammatory responses (Chan and Gack, 2015; Liu et al., 2015). Further study should be carried out to clarify this important issue.

In short, we characterized a MAVS ortholog from the Chinese tree shrew and confirmed the conservation of the MAVS structure and function in this species. Further characterization of tMAVS-mediated antiviral signaling pathway in the tree shrew will be rewarding as this animal has the potential to be used for creating animal models for viral infection (Li et al., 2014; Zheng et al., 2014) and has unique genetic features in immune system (Fan et al., 2013).

Acknowledgements

We thank Dr. Xinwen Chen for providing SeV and VSV, Dr. Jumin Zhou for providing HSV-1, and Dr. Hui Zheng for providing ISRE-Luc promoter vector. We are grateful to Mr. Ronghua Luo, Mr. Yong Wu for technical assistance. This study was supported by the National Natural Science Foundation of China (U1402224), the National 863 Project of China (2012AA021801) and grants from the Chinese Academy of Sciences (KSCX2-EW-R-11).

Conflict of interests

The authors declared no conflicts of interests.

References

Amako, Y., Tsukiyama-Kohara, K., Katsume, A., Hirata, Y., Sekiguchi, S., Tobita, Y., et al., 2010. Pathogenesis of hepatitis C virus infection in *Tupaia belangeri*. J. Virol. 84, 303–311.

Belgnaoui, S.M., Paz, S., Hiscott, J., 2011. Orchestrating the interferon antiviral response through the mitochondrial antiviral signaling (MAVS) adapter. Curr. Opin. Immunol. 23, 564–572.

Biacchesi, S., LeBerre, M., Lamoureux, A., Louise, Y., Lauret, E., Boudinot, P., et al., 2009. Mitochondrial antiviral signaling protein plays a major role in induction of the fish innate immune response against RNA and DNA viruses. J. Virol. 83, 7815–7827.

Chan, Y.K., Gack, M.U., 2015. RIG-I-like receptor regulation in virus infection and immunity. Curr. Opin. Virol. 12C, 7–14.

Dixit, E., Boulant, S., Zhang, Y., Lee, A.S., Odendall, C., Shum, B., et al., 2010. Peroxisomes are signaling platforms for antiviral innate immunity. Cell 141, 668–681.

Edgar, R.C., 2004. MUSCLE: multiple sequence alignment with high accuracy and high throughput. Nucleic Acids Res. 32, 1792–1797.

Fan, Y., Huang, Z.-Y., Cao, C.-C., Chen, C.-S., Chen, Y.-X., Fan, D.-D., et al., 2013. Genome of the Chinese tree shrew. Nat Commun. 4, 1426.

Fan, Y., Yu, D., Yao, Y.-G., 2014. Tree shrew database (TreeshrewDB): a genomic knowledge base for the Chinese tree shrew. Sci. Rep. 4, 7145.

Horner, S.M., Liu, H.M., Park, H.S., Briley, J., Gale, M., Jr., 2011. Mitochondrial-associated endoplasmic reticulum membranes (MAM) form innate immune synapses and are targeted by hepatitis C virus. Proc. Natl. Acad. Sci. U.S.A. 108, 14590–14595.

Iwamura, T., Yoneyama, M., Yamaguchi, K., Suhara, W., Mori, W., Shiota, K., *et al.*, 2001. Induction of IRF-3/-7 kinase and NF-κB in response to double-stranded RNA and virus infection: common and unique pathways. Genes Cells 6, 375–388.

Kato, H., Takeuchi, O., Sato, S., Yoneyama, M., Yamamoto, M., Matsui, K., et al., 2006. Differential roles of MDA5 and RIG-I helicases in the recognition of RNA viruses. Nature 441, 101–105.

Kawai, T., Takahashi, K., Sato, S., Coban, C., Kumar, H., Kato, H., et al., 2005. IPS-1, an adaptor triggering RIG-I- and Mda5-mediated type I interferon induction. Nat. Immunol. 6, 981–988.

Kock, J., Nassal, M., MacNelly, S., Baumert, T.F., Blum, H.E., von Weizsacker, F., 2001. Efficient infection of primary *tupaia* hepatocytes with purified human and woolly monkey hepatitis B virus. J. Virol. 75, 5084–5089.

Li, J.-P., Liao, Y., Zhang, Y., Wang, J.-J., Wang, L.-C., Feng, K., et al., 2014. Experimental infection of tree shrews (*Tupaia belangeri*) with Coxsackie virus A16. Zool Res. 35, 485–491.

Liniger, M., Summerfield, A., Zimmer, G., McCullough, K.C., Ruggli, N., 2012. Chicken cells sense influenza A virus infection through MDA5 and CARDIF signaling involving LGP2. J. Virol. 86, 705–717.

Liu, X., Wang, Q., Pan, Y., Wang, C., 2015. Sensing and responding to cytosolic viruses invasions: an orchestra of kaleidoscopic ubiquitinations. Cytokine Growth Factor Rev. doi:10.1016/j.cytogfr.2015.03.001.

Meylan, E., Curran, J., Hofmann, K., Moradpour, D., Binder, M., Bartenschlager, R., *et al.*, 2005. Cardif is an adaptor protein in the RIG-I antiviral pathway and is targeted by hepatitis C virus. Nature 437, 1167–1172.

Peng, Y.Z., Ye, Z.Z., Zou, R.J., Wang, Y.X., Tian, B.P., Ma, Y.Y., et al., 1991. Biology of Chinese Tree Shrews (*Tupaia belangeri chinensis*). Yunnan Science and Technology Press, Kunming, China.

Potter, J.A., Randall, R.E., Taylor, G.L., 2008. Crystal structure of human IPS-1/MAVS/VISA/Cardif caspase activation recruitment domain. BMC Struct. Biol. 8, 11.

Rosen, A., Gelderblom, H., Darai, G., 1985. Transduction of virulence in herpes simplex virus type 1 from a pathogenic to an apathogenic strain by a cloned viral DNA fragment. Med Microbiol Immunol. 173, 257–278.

Seth, R.B., Sun, L., Ea, C.K., Chen, Z.J., 2005. Identification and characterization of MAVS, a mitochondrial antiviral signaling protein that activates NF-κB and IRF 3. Cell 122, 669–682.

Simora, R.M., Ohtani, M., Hikima, J., Kondo, H., Hirono, I., Jung, T.S., et al., 2010. Molecular cloning and antiviral activity of *IFN-β promoter stimulator-1 (IPS-1)* gene in Japanese flounder, *Paralichthys olivaceus*. Fish Shellfish Immunol. 29, 979–986.

Su, J., Huang, T., Yang, C., Zhang, R., 2011. Molecular cloning, characterization and expression analysis of *interferon-β promoter stimulator 1 (IPS-1)* gene from grass carp *Ctenopharyngodon idella*. Fish Shellfish Immunol. 30, 317–323.

Takeuchi, O., Akira, S., 2010. Pattern recognition receptors and inflammation. Cell 140, 805–820.
Tamura, K., Peterson, D., Peterson, N., Stecher, G., Nei, M., Kumar, S., 2011. MEGA5: molecular evolutionary genetics analysis using maximum likelihood, evolutionary distance, and maximum parsimony methods. Mol. Biol. Evol. 28, 2731–2739.
Tamura, T., Yanai, H., Savitsky, D., Taniguchi, T., 2008. The IRF family transcription factors in immunity and oncogenesis. Ann Rev Immunol. 26, 535–584.
Wang, D., Fang, L., Li, T., Luo, R., Xie, L., Jiang, Y., et al., 2008. Molecular cloning and functional characterization of porcine IFN-β promoter stimulator 1 (IPS-1). Vet. Immunol. Immunopathol. 125, 344–353.
Wang, W.-G., Huang, X.-Y., Xu, J., Sun, X.-M., Dai, J.-J., Li, Q.-H., 2012. Experimental studies on infant *Tupaia belangeri chineses* with EV71 infection. Zool Res. 33, 7–13.
Xu, H., He, X., Zheng, H., Huang, L.J., Hou, F., Yu, Z., et al., 2014. Structural basis for the prion-like MAVS filaments in antiviral innate immunity. eLife 3, e01489.
Xu, L., Fan, Y., Jiang, X.-L., Yao, Y.-G., 2013a. Molecular evidence on the phylogenetic position of tree shrews. Zool Res. 34, 70–76.
Xu, L., Zhang, Y., Liang, B., Lv, L.-B., Chen, C.-S., Chen, Y.-B., et al., 2013b. Tree shrews under the spot light: emerging model of human diseases. Zool Res. 34, 59–69.
Xu, L.G., Wang, Y.Y., Han, K.J., Li, L.Y., Zhai, Z., Shu, H.B., 2005. VISA is an adapter protein required for virus-triggered IFN-beta signaling. Mol. Cell 19, 727–740.
Xu, X., Chen, H., Cao, X., Ben, K., 2007. Efficient infection of tree shrew (*Tupaia belangeri*) with hepatitis C virus grown in cell culture or from patient plasma. J. Gen. Virol. 88, 2504–2512.
Yan, R.Q., Su, J.J., Chen, Z.Y., Liu, Y.G., Gan, Y.Q., Zhou, D.N., 1984. A preliminary study on experimental infection of human hepatitis B virus in adult tree shrews. J. Guangxi Med. Univ. 1, 10–15.
Yan, R.Q., Su, J.J., Huang, D.R., Gan, Y.C., Yang, C., Huang, G.H., 1996. Human hepatitis B virus and hepatocellular carcinoma. I. Experimental infection of tree shrews with hepatitis B virus. J. Cancer Res. Clin. Oncol. 122, 283–288.
Yang, Z.F., Zhao, J., Zhu, Y.T., Wang, Y.T., Liu, R., Zhao, S.S., et al., 2013. The tree shrew provides a useful alternative model for the study of influenza H1N1 virus. Virology 10, 111.
Yu, D., Xu, L., Liu, X.-H., Fan, Y., Lü, L.-B., Yao, Y.-G., 2014. Diverse interleukin-7 mRNA transcripts in Chinese tree shrew (*Tupaia belangeri chinensis*). PLoS ONE 9, e99859.
Zheng, Y.-T., Yao, Y.-G., Xu, L., 2014. Basic Biology and Disease Models of Tree Shrews. Yunnan Science and Technology Press, Kunming, China.
Zhong, B., Yang, Y., Li, S., Wang, Y.-Y., Li, Y., Diao, F., et al., 2008. The adaptor protein MITA links virus-sensing receptors to IRF3 transcription factor activation. Immunity 29, 538–550.